

## JET PRODUCTION AND THE DYNAMICAL ROLE OF COLOR\*

Stanley J. Brodsky  
Stanford Linear Accelerator Center  
Stanford University, Stanford, California 94305



**Abstract:** We discuss how multiparticle jets which originate from quarks, multiquarks, hadrons, or gluons can be distinguished by their (a) quantum number retention, (b) leading particle distributions, and (c) hadronic multiplicity. The possible quantitative connection between initial color separation and hadron multiplicity is emphasized. Evidence for wee quark exchange as a dominant hadronic mechanism is presented. We also discuss several new mechanisms for gluon jet production. Finally, we consider the possibility of utilizing a high multiplicity trigger to expose gluon exchange and production contributions in hadron- and lepton-induced reactions.

**Résumé:** Nous discutons comment les jets de multiparticules dont l'origine est soit des quarks, des multiquarks des hadrons ou des gluons peuvent être distingués par (a) leur retention de nombres quantiques (b) leurs distributions de particules dominantes (c) leur multiplicité hadronique. Nous mettons l'accent sur la liaison quantitative possible entre la séparation des couleurs initiales et la multiplicité hadronique. L'évidence pour l'échange de wee quarks comme un mécanisme hadronique dominant est présentée. Nous discutons aussi plusieurs nouveaux mécanismes pour la production de jet engendré par un gluon. Finalement, nous considérons la possibilité d'utiliser la détection d'évènements de haute multiplicité pour mettre en évidence les contributions des échange et production de gluons dans les réactions induites par des hadrons et des leptons.

---

\*Work supported by the Energy Research and Development Administration.

## I. Introduction

The production of multiparticle jets appears to be a common feature of all high energy hadron- and lepton-induced reactions.<sup>1</sup> Despite the indications that their average multiplicity<sup>2</sup>  $\langle n \rangle$  and transverse momentum distributions are surprisingly similar, the underlying quark and gluon content of these jets can be quite diverse. In particular, we expect quark fragmentation jets of various flavors in  $e^+e^- \rightarrow \text{hadrons}$ , as well as in the current fragmentation region of lepton-induced reactions. We also expect di-quark ( $q\bar{q}$ ) and multiquark jets in the target fragmentation region in deep inelastic scattering as well as in the beam and target region in Drell-Yan massive pair production. In the case of large  $p_T$  reactions, one expects quark, multiquark, and even jets of hadronic parentage depending on the hard scattering subprocess. Even more intriguing, if one takes quantum chromodynamics at face value, one must expect at some level, the production of jets corresponding to gluon fragmentation in any of these processes. In the case of ordinary forward hadronic reactions, the jet-like forward and backward multiparticle systems are usually considered to have a conventional hadronic origin, but as we shall discuss in Sections VI and VII, the primary parents of these systems could well be colored, if the initial hadronic interaction can be identified as being due to gluon or quark exchange.

One of the important phenomenological questions in particle physics, then, is how to empirically discriminate between jets of different origin, i.e., how to distinguish the different flavor, color, number of quarks or gluons of their parent systems. In this paper I will discuss a number of discriminants, including  $dn/dy$  (the height of the rapidity plateau in the central region) (Section VII), the fragmentation properties (the power-law falloff and quantum numbers of leading particles at  $x \rightarrow 1$ ) (Section IV), and the possible retention of charge and other quantum numbers (Section II). The multiquark jet which is left behind in the target fragmentation region in deep inelastic scattering and the Drell-Yan process is especially interesting because of theoretical uncertainties regarding the composition of the hadron's parton wavefunction. We discuss special tests for such systems in Section II. Finally, in Section VII we speculate on the possibility that the initial color separation controls the height of the multiplicity plateau, and that events with large multiplicities are sensitive to gluon exchange contributions.

## II. Charge Retention by Quark and Multiquark Systems<sup>3</sup>

Feynman<sup>4</sup> originally proposed the elegant ansatz that the total charge of a jet

$$\langle Q \rangle_J = \sum_{h \in J} Q_h \int_0^1 \frac{dn_h/J}{dx} dx = \sum_{h \in J} Q_h \int_{y_0}^{y_{\max}} \frac{dn_h/J}{dy} dy \quad (2.1)$$

could reflect, in the mean, the charge of its parent. However, as noted by Farrar and Rosner,<sup>5</sup> this connection can fail in specific model calculations, and accordingly there has been little subsequent interest in using this method as a jet discriminant.

In order to see why exact charge reten-

tion fails, consider the simple model for

$e^+ e^- \rightarrow \gamma \rightarrow q\bar{q} \rightarrow$  hadrons shown in Fig. 1. The rapidity interval  $|y| < y_{\max} \sim \frac{1}{2} \log s$  is filled uniformly by the production of neutral gluons,

which subsequently decay to  $q\bar{q}$  pairs. These then recombine with the leading quarks to produce mesons. If we could cut through a

meson and sum all the charges to the right of the point  $y_a$ , then clearly  $Q_J(y > y_a) = Q_{\bar{q}}$ . However, since we must sum over hadron charges an extra quark is always included in the sum, and the total charge corresponding to the antiquark jet is<sup>3,5</sup>

$$\langle Q \rangle_J = Q_{\bar{q}} + \eta_Q \quad (2.2)$$

where  $\eta_Q = \langle Q_q \rangle_{\text{sea}}$  is the mean charge of quarks in the sea:  $\eta_Q = \frac{1}{2}(2/3 - 1/3) = 1/6$  for an SU(2)- (or SU(4)-) symmetric sea, and  $\eta_Q = \frac{1}{3}(2/3 - 1/3 - 1/3) = 0$  for an SU(3)-symmetric sea. Actually this result is quite model-independent, and Eq. (2.2) will apply to all jets which need a quark for neutralization. More generally, for any conserved charge  $\Lambda = I_Z$ ,  $B$ ,  $S$ , etc., one predicts<sup>3,5</sup>

$$\langle \Lambda \rangle_J = \Lambda_J \pm \eta_\Lambda \quad (2.3)$$

where  $\Lambda_J$  is the quantum number of the parent quark or multiquark system and the sign is  $+$  ( $-$ ) if the parent needs a quark (antiquark) to neutralize it. Notice that  $\eta_\Lambda$  is independent of the process and of the jet type and is a universal number.<sup>3</sup> The result (2.3) is unaffected by resonance decay or baryon production. From parametrizations<sup>6</sup> of the quark

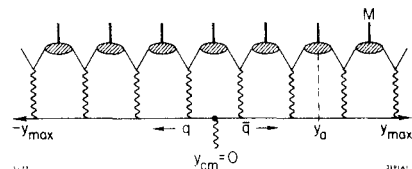


Fig. 1. Simplified model for the rapidity distribution of virtual gluons and mesons in  $e^+ e^- \rightarrow q\bar{q} \rightarrow$  hadrons. See also Section III.

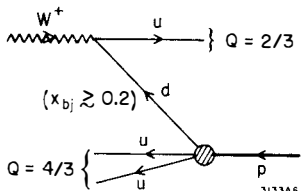


Fig. 2. Parton model diagram for  $\nu p \rightarrow \mu^- X$  as viewed in the  $W^+ p$  c.m. system for the valence region ( $x_{bj} \gtrsim 0.2$ ).

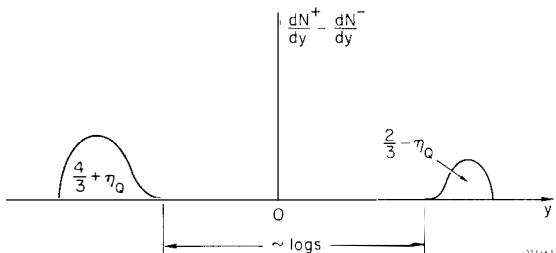


Fig. 3. Idealized distribution for  $W^+ p \rightarrow X$  ( $\nu p \rightarrow \mu^- X$ ) as  $s \rightarrow \infty$ .

distribution functions, one can already determine empirically that  $\eta_Q \approx 0.07$ , corresponding to partial suppression of the strange and heavy quarks in the sea. For the usual quark models,  $\eta_B = \frac{1}{3}$ ,  $\eta_{L_Z} = 0$ .

Given the fact that the  $\eta_\Lambda$  are universal numbers which can be established empirically, quantum number retention can be a viable method for identifying specific quark and multiquark systems. For example, Fig. 2 shows the expected initial quark flow in the  $W^+ p$  c.m. system for  $\nu p \rightarrow \mu^- X$ , in the valence quark region  $x_{bj} \gtrsim 0.2$ , and Fig. 3 indicates the predicted hadronic charge distribution  $dN^+/dy - dN^-/dy$  expected at very large  $s = (q+p)^2$ . For  $x_{bj} < 0.2$ , the presence of sea quarks which can be hit by the  $W^+$  tends to further increase the asymmetry between the two hemispheres. Taking

$\eta_Q = 0.07$ , this implies that the plateau height will be  $\gtrsim 2.3$  times larger in the target ( $uu$ ) fragmentation region compared to the current ( $u$ ) fragmentation region. The data<sup>7</sup> (Fig. 4a)

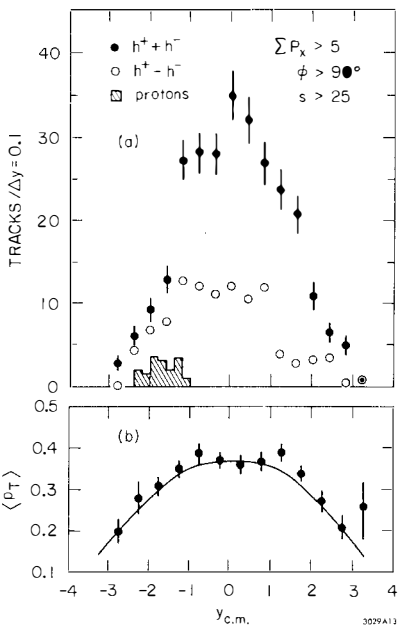


Fig. 4. Data from the Fermilab 15 ft bubble chamber for  $\nu p \rightarrow \mu^- X$ .<sup>7</sup> The rapidity distribution and the charge structure  $dN^+/dy - dN^-/dy$  of the final state are shown, as well as the transverse momentum distribution of the emitted hadrons. The curve for  $\langle p_T(y) \rangle$  is from  $pp$  reactions.

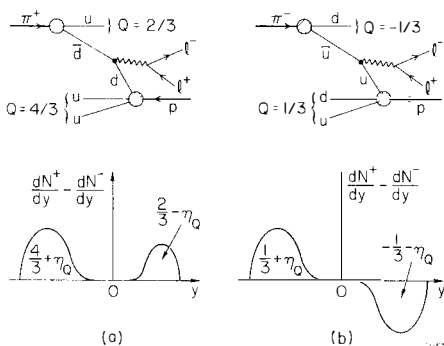


Fig. 5. The Drell-Yan mechanism and the expected charge distribution for  $\pi^+ p \rightarrow l^+ l^- + X$  in the valence-valence region ( $x_\pi, x_p \gtrsim 0.2$ ).

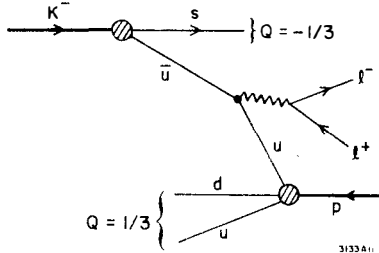


Fig. 6. The Drell-Yan mechanism for  $K^- p \rightarrow l^+ l^- + X$  in the valence-valence region ( $x_K, x_p \gtrsim 0.2$ ).

seem consistent with this prediction. It is also interesting to note that the transverse momentum distribution of  $W^+$ -induced events is the same as that measured in  $pp$  collisions, shown by the solid lines in Fig. 4b.

One of the most interesting areas of application of the charge retention technique is to confirm the underlying quark structure predicted by the Drell-Yan process.<sup>8</sup> For example consider  $\pi^+ p \rightarrow l^+ l^- + X$  in the valence quark region ( $x_a, x_b \gtrsim 0.2$ ;  $x_a - x_b \cong x_L$ ,  $x_a x_b \cong M^2/s$ ). The predicted quark-flow diagrams and the charge distribution of the final state hadrons are shown in Fig. 5. We estimate that the width of the charged fragmentation regions is  $\sim 2-3$  units in rapidity so very large  $s$  is needed to make a clear separation. Even at moderate  $s$ , though, one can study the ratio of the charge-difference plateau heights.

Because of the high energies available, and the possibility of controlling the momentum fractions  $x_a$  and  $x_b$ , systematic measurements of the hadron fragmentation region in the Drell-Yan process can lead to essential information on the complete hadron wavefunction in both the wee and valence quark domain. For example, the expected charge distribution in the valence region for  $K^- p \rightarrow l^+ l^- + X$  is shown in Figs. 6 and 7. As in the previous examples, we assume that the (uud) Fock space wavefunction is the dominant component in the proton at large  $x_{bj}$ , and that the rapidities of the spectator u and d quarks are nearly equal to the initial rapidity. If we now consider events with  $x_b$  small

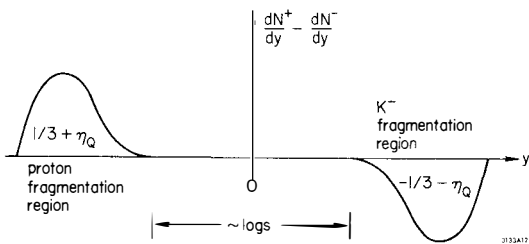


Fig. 7. The expected distribution of charge in rapidity for the process of Fig. 6.

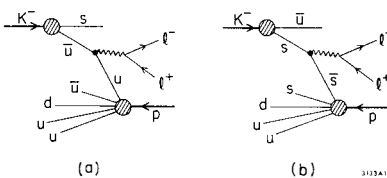


Fig. 8. The Drell-Yan mechanism for  $K^- p \rightarrow l^+ l^- X$  in the "valence-sea" region ( $x_K \gtrsim 0.2$ ,  $x_p \lesssim 0.2$ ).

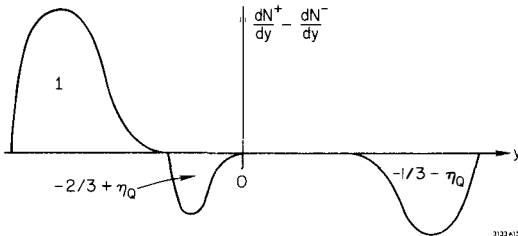


Fig. 9. The expected distribution of charge in rapidity for the process of Fig. 6 in the "hole fragmentation" model.

or wee, diagrams 8a and 8b become important (with a dominant because  $Q_u^2 = 4Q_s^2$ ). In models where the extra  $u\bar{u}$  pair is created from a neutral system, e.g., from gluon decay as in Ref. 9, then the wee quark charge is compensated locally in rapidity, and one expects the charge distribution shown in Fig. 9. This is also the prediction of the "hole" fragmentation model of Bjorken<sup>10</sup> and Feynman.<sup>4</sup> On the other hand, the charge distribution of the proton fragments may be more homogeneous, since it is possible that the interacting wee quarks are constituents of virtual charged and neutral mesons, as suggested in Ref. 11. The same result is predicted if we assume that the bound quarks of the spectator

system exchange momentum and tend to equalize their velocities.<sup>12</sup> The resulting charge distribution would thus resemble Fig. 10. Thus detailed measurements of the charge flow in the hadron fragmentation regions could well distinguish between these basic theoretical models. Comparison between the Drell-Yan process,  $\psi$  production, and ordinary collisions should be illuminating.

Other tests of charge and quantum number retention, especially in  $e^+ e^-$  annihilation, are discussed in Ref. 3.

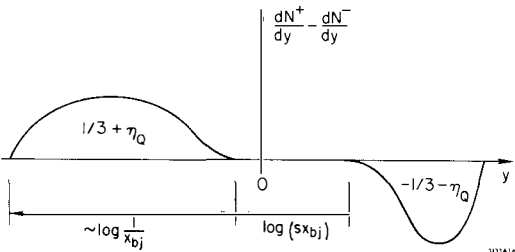


Fig. 10. An alternate possibility for the distribution of charge in rapidity for the process of Fig. 8.

### III. A Model for Jet Fragmentation<sup>3</sup>

One of the basic uncertainties in the quark model is the nature of the space-time evolution of the final state hadrons. In constructing a model one must keep in mind that (aside from resonance decay) the emission of one hadron cannot cause nor directly influence the emission of other hadrons, since they are at a space-like separation. A simple model for  $e^+e^- \rightarrow$  hadrons, which is a realization of Bjorken's inside-outside cascade mechanism,<sup>10</sup> is shown in Fig. 11. After the  $q\bar{q}$  begin to separate, (virtual) gluons are emitted with flat distribution in rapidity. One assumes that each gluon lives, on the average, a characteristic proper time  $\tau = 1/d$ , producing quarks and antiquarks which recombine to form color singlet mesons. The hadron production then occurs near the hyperboloid,  $t^2 - x^2 = d^2$ , which meets the quark world line at  $t \sim \gamma d$ . The initial quark and antiquark are thus free for a time  $t \propto \sqrt{s}$  which justifies them as being treated as free particles in the calculation of the annihilation cross section. In the  $e^+e^-$  center-of-mass frame, the fastest mesons are emitted last.<sup>13</sup>

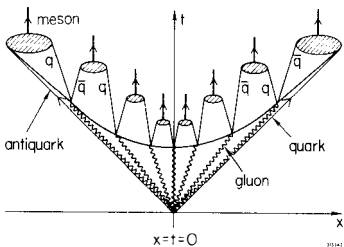


Fig. 11. Space-time evolution of the hadronic final state in  $e^+e^-$  annihilation. The initial  $q\bar{q}$  pair is produced at  $x=t=0$  and the hadrons are produced near the hyperboloid,  $t^2 - x^2 = d^2$ . The transverse direction is not shown in the diagram.

Although this model is grossly oversimplified, it is causal and covariant and has many characteristics expected in gauge theories and jet production. Resonance and baryon production can also be included. The model can serve as a simple testing ground for the effects of quark mass and valence effects, etc. An application is the quantum

number retention rule, Eq. (2.3). Further, in this simple model the meson multiplicity is roughly equal to the gluon multiplicity and grows logarithmically. We discuss this feature further in the color model of Section VI.

#### IV. Leading Particle Behavior

In addition to its retained quantum numbers an important discriminant of a jet is the  $x \rightarrow 1$  behavior of its leading particles. The basic idea is as follows: consider a fast moving composite system A with a large momentum  $\vec{p}_A \parallel z$ . See Fig. 12a. The probability that one constituent (or subset of constituents) a, in a virtual state, has nearly all the momentum of A must vanish rapidly as the remaining constituents, the  $n(\bar{a}A)$  spectators, are forced to low momentum. In fact, assuming an underlying scale-invariant model one finds<sup>14</sup>

$$G_{a/A}(x) = \frac{dN_{a/A}(x)}{dx} \xrightarrow{x \rightarrow 1} C(1-x)^{2n(\bar{a}A) - 1} \quad (4.1)$$

where  $x$  is the light cone momentum fraction,  $x = (p_0^a + p_z^a) / (p_0^A + p_z^A)$ . This result for the probability distribution leads to the predictions  $\nu W_{2p} \sim G_{q/p}(x) \sim (1-x)^3$ ,  $\nu W_{2\pi} \sim (1-x)$ ,  $G_{\pi/q} \sim (1-x)^7$ ,  $G_{\bar{q}/p} \sim (1-x)^7$ ,  $G_{M/B} \sim (1-x)^5$ , etc. Comparisons with experiment, corrections and other modifications are discussed in Ref. 1.

An immediate application of the counting rule (4.1) is the prediction of the  $x_L = p_z^{\text{c.m.}} / p_{z \text{ max}}^{\text{c.m.}}$  dependence of the forward inclusive cross section for the dissociation of a composite system. For example, one predicts

for fast nuclear collisions (see Fig. 12b)

$$\frac{1}{\sigma} \frac{d\sigma}{dx_L} (A + B \rightarrow p + X) \sim (1-x_L)^{6(A-1)-1} \quad (4.2)$$

and

$$\frac{1}{\sigma} \frac{d\sigma}{dx_L} (A + B \rightarrow A' + X) \sim (1-x_L)^{6(A-A')-1} \quad (4.3)$$

since there are  $3(A-A')$  quark spectators forced to low momentum. These and other predictions have recently been shown in a beautiful analysis by Schmidt and Blankenbecler<sup>15</sup> to be in striking

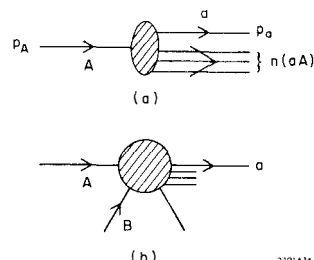


Fig. 12. (a) Fragmentation of A into a subset of constituent a. The number of elementary constituent spectators is  $n(\bar{a}A)$ . (b) Fragmentation of  $A + B \rightarrow a + X$ .

agreement with measurements of deuteron, alpha, and carbon dissociation at LBL. The prediction  $G_{p/d} \sim (1-x)^5$  is also consistent with the Fermi motion observed in measurements of  $ed \rightarrow epn$  for  $x = -q^2/2p_d \cdot q \sim 1$ .<sup>16</sup>

One of the most intriguing applications<sup>17</sup> of the counting rule (4.1) is to forward inclusive hadron reactions  $pp \rightarrow \pi X$ , etc. For  $x_L \rightarrow 1$  this is normally considered the domain of the triple Regge mechanism, where  $d\sigma/dx (A + B \rightarrow C + X) \sim (1-x)^{1-2\alpha(t)}$ . However, in the range  $0.2 < x_L < 0.8$  the measured cross sections<sup>18</sup> appear to have  $p_T$ -independent powers of  $(1-x)$  (especially when parametrized in terms of  $x_R = p_{\text{c.m.}}^{\text{c.m.}}/p_{\text{max}}^{\text{c.m.}}$ ) and is thus more suggestive of a fragmentation mechanism.

At this point we shall distinguish three possible fragmentation models for high energy hadron collisions<sup>19</sup>:

(1) The incoming beam is dissociated by the Pomeron.<sup>17</sup> Then as in Eq. (4.1)  $d\sigma/dx (A + B \rightarrow C + X) \sim (1-x_C)^{2n(\bar{C}A)-1}$ ; i.e., the fragmenting jet is the excited hadron A. (Although  $x_C$  is defined as the light-cone variable,  $x_C = x_R$  should be sufficiently accurate.)

(2) Inelastic collisions begin with the exchange of a color gluon, as in the Low<sup>20</sup>-Nussinov<sup>21</sup> model. See Fig. 15e'. The fragmenting jet is then an octet  $(A)_8$  with the same quark structure as A. Again, one predicts the same distribution as in (1), if  $C \neq A$ .

(3) Inelastic collisions begin with the exchange (or annihilation) of a wee quark, as in the Feynman wee parton model, as in Fig. 15e. The fragmenting jet then has one fewer spectator compared to the gluon or dissociation mechanisms. We thus have<sup>19</sup>

$$d\sigma/dx (A + B \rightarrow C + X) \sim (1-x_C)^{2n(\bar{C}A)-3} . \quad (4.4)$$

For example, for  $pp \rightarrow \pi^+ X$ , the  $\pi^+$  can be formed from the five-quark  $|duudd\rangle$  Fock-state component of the proton. The Pomeron or gluon excitation models (1) and (2) then give  $d\sigma/dx \sim (1-x)^5$ , corresponding to three spectators (dud), whereas wee quark exchange (3) gives  $d\sigma/dx \sim (1-x)^3$ . The ISR data<sup>18</sup> for  $pp \rightarrow \pi^+ X$  is consistent with  $(1-x_\pi)^{3.1}$  for  $p_T < 0.85$  GeV,  $0.4 < x < 0.9$  when fit using the variable  $x_R = p_{\text{c.m.}}^{\text{c.m.}}/p_{\text{max}}^{\text{c.m.}}$ , or  $(1-x_L)^{3.5}$  when fit using  $x_L = p_z^{\text{c.m.}}/p_{z \text{ max}}^{\text{c.m.}}$ . This then gives support to the quark exchange picture. We discuss further consequences of this model for hadron multiplicities in Sections VI and VII.

Predictions for particle ratios are independent of which mechanism (1)-(3) is assumed. For example, just by counting the extra quark spectators one predicts  $(pp \rightarrow K^- X)/(pp \rightarrow K^+ X) \sim (1-x_K)^4$  and  $(pp \rightarrow \bar{\Lambda} X)/(pp \rightarrow \Lambda X) \sim (1-x_L)^8$  which appears to be not inconsistent with experiment.<sup>18</sup> One also can predict ratios for different beams for massive lepton pair and  $\psi$  production. These and other applications are discussed in Ref. 19.

If the quark exchange or annihilation mechanism (3) is actually correct then there can be a remarkable, long-range correlation set up in double-fragmentation reactions. For example in  $pp \rightarrow \pi_{(1)}^+ \pi_{(2)}^+ X$ , with fast pions in the forward and backward direction, the requirement of quark exchange or  $q\bar{q}$  annihilation forces an extra pair of spectators. One then predicts  $d\sigma/dx_1 dx_2 (pp \rightarrow \pi_{(1)}^+ \pi_{(2)}^+ X) \sim (1-x_1)^3 (1-x_2)^7 + (x_1 \leftrightarrow x_2)$ . This feature of the model and further examples are discussed in detail in a recent paper by Gunion and myself.<sup>19</sup>

## V. How to See a Gluon Jet

Thus far in this talk, the emphasis has been on quark and multiquark jets. It is apparent that at some level QCD must imply the existence of gluon jets. Several essentially scale-invariant processes have been suggested to find such systems. For example, the subprocess  $e^+ e^- \rightarrow q\bar{q}g$  (see Fig. 15c') leads to a coplanar three-jet configuration,<sup>22</sup> and the reaction  $\gamma^* q \rightarrow q\bar{q}g$  leads to a double jet structure in the current fragmentation region of deep inelastic electroproduction.<sup>23</sup> However, the background from constituent interchange model processes such as  $e^+ e^- \rightarrow q\bar{q}M$  and  $\gamma^* q \rightarrow Mq$  is severe until very large  $p_T$  and  $\sqrt{s}$ ; this is discussed in detail by DeGrand, Ng, and Tye.<sup>24</sup> Gluon jets, of course, may also be predicted in high  $p_T$  reactions from  $gg \rightarrow gg$ ,  $Mq \rightarrow gq$ , etc.<sup>25, 26</sup>

Recently Caswell, Horgan, and I<sup>26</sup> have considered several processes which must have a lower limit for gluon jet production if  $\alpha_s \neq 0$ . For example, by comparing contributions the subprocesses  $q\bar{q} \rightarrow \gamma^* \rightarrow \mu^+ \mu^-$  for large  $p_T$  single muons and  $q\bar{q} \rightarrow \gamma g$  for large  $p_T$  (real or virtual) photons, we can derive a lower bound for scale-invariant hard photon production (see Fig. 13),<sup>26</sup>

$$\frac{Ed\sigma/d^3p (pp \rightarrow \gamma X)}{Ed\sigma/d^3p (pp \rightarrow \mu^+ \mu^-)} = \frac{\frac{4}{3} \alpha_s}{\alpha} \frac{4}{\langle \sin^2 \hat{\theta} \rangle} \quad (4.1)$$

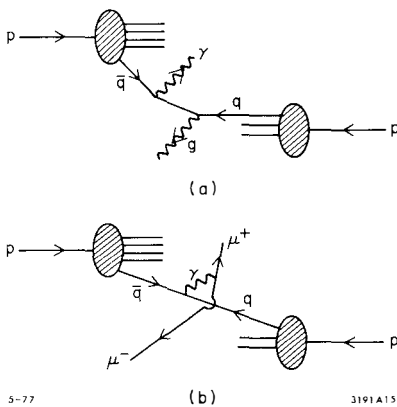


Fig. 13. (a) Contribution of the  $q\bar{q} \rightarrow \mu^+ \mu^-$  subprocess to  $\mu^+ \mu^-$  production at large  $p_T$ . (b) Contribution of  $q\bar{q} \rightarrow \gamma\gamma$  to real or virtual photon production at large  $p_T$ .

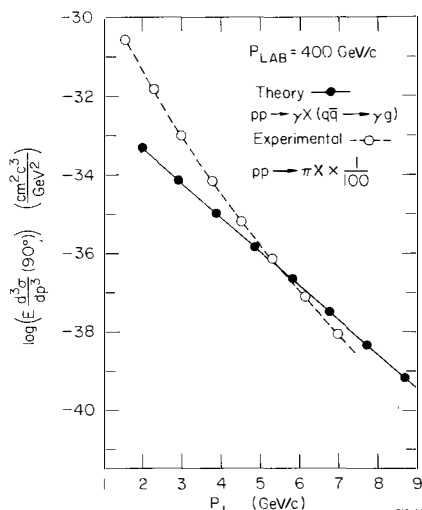


Fig. 14. Predicted contribution  $E d\sigma/d^3p$  ( $pp \rightarrow \gamma X$ ) at  $p_{\text{lab}} = 400 \text{ GeV}/c$ ,  $\theta_{\text{c.m.}} = 90^\circ$  from the scale-invariant subprocess ( $q\bar{q} \rightarrow \gamma g$ ). For reference, the Chicago-Princeton data of Cronin et al. for  $pp \rightarrow \pi X$  is shown multiplied by a vector meson dominant factor of  $10^{-2}$ . From Ref. 26.

where  $\hat{\theta}$  is the c.m. angle of the subprocess. This result should be applicable for  $p_T \gtrsim 4 \text{ GeV}$ , where the  $q\bar{q} \rightarrow \mu^+ \mu^-$  subprocess dominates the single muon cross section. Notice that all the uncertainties from the  $q$  and  $\bar{q}$  distributions cancel in this ratio. The predicted cross section for  $\alpha_s = 0.25$  and an estimated background from vector dominance terms are shown in Fig. 14. When the subprocess  $q\bar{q} \rightarrow \gamma g$  dominates, a gluon jet is predicted on the away side of the direct photon, although other subprocesses such as  $qg \rightarrow q\gamma$  can also contribute here.

In general, any collision that produces direct (real or virtual) hard photons, e.g.,  $pp \rightarrow \gamma + X$ ,  $e^+ e^- \rightarrow \gamma + X$ ,  $ep \rightarrow e\gamma + X$ , etc., will also produce a gluon jet with a cross section from the substitution  $\alpha \rightarrow \frac{4}{3} \alpha_s$ .<sup>26</sup> A useful way to verify the hard photon-quark current coupling in  $e^+ e^- \rightarrow q\bar{q}\gamma$  and  $eq \rightarrow e\gamma q$  is to measure the charge asymmetry in  $e^+ e^- \rightarrow \gamma h^\pm X$ , and  $e^\pm p \rightarrow e^\pm \gamma X$  as discussed in Ref. 27.

A gluon jet may be identified from the global neutral character of its quantum numbers, and relative to quarks, the suppression of leading fragments. For example, one expects  $G_{\pi/q}(x)/G_{\pi/g}(x) \sim \alpha_s(1-x) \log s/mq^2$  where the nonscaling factor is due to the  $\Delta k_T^2/k_T^2$  falloff of the  $q\bar{q}g$  coupling. However,

the most important discriminant of a gluon jet may be its hadron multiplicity density  $dN/dy$  in the central rapidity region. We discuss this possibility in the next sections.

## VI. The Dynamics of Color Separation

One of the central questions in the quark-gluon description of hadron dynamics is the question of what controls the magnitude and energy dependence of hadron production. In a recent paper, Gunion and I<sup>12</sup> considered the possibility that the multiplicity distribution at high energies depends in a quantitative way on the color separation initially set up in the collision. In quantum electrodynamics, soft photons arise via bremsstrahlung from initial or final charged lines, and the average multiplicity is computed from the sum over all charged-particle pairs, each contribution depending on the product of their charges and a function which increases with the relative rapidity separation of the pair. In the analogous case of quantum chromodynamics, charge is replaced by color, and the hadrons—which are color singlets—do not radiate. Radiation of colored gluons occurs only when two colored objects (e.g., virtual quarks) are separated in rapidity. In addition there is a natural infrared cutoff determined by the size of the confinement region of color. We presume that the radiated color gluons eventually materialize as hadrons in such a way that the hadron multiplicity is a direct, monotonic function of the rising gluon multiplicity and hence only depends on the separating color currents. (A model where this relationship is linear is discussed in Section III.) Two processes with the same initial color-current configuration will thus produce the same multiplicity in the central rapidity region. (The principal effect of quark flavor will be to influence the quantum numbers of the leading hadrons.) The separation of color together with the eventual confinement of color thus leads naturally to a rising hadron multiplicity.

In the canonical case,  $e^+ e^- \rightarrow$  hadrons, the electromagnetic current produces at time = 0 a quark-antiquark pair, and there is an initial separation of color 3 and  $\bar{3}$ . Eventually the systems are neutralized and produce hadron jets, as in the model described in Section III. It is evident from the structure of QCD that the gluon radiation depends on the magnitude of the color charge and the rapidity separation of the  $q$  and  $\bar{q}$  systems, and that it is flavor-independent; i.e., for the same rapidity separation the central hadron multiplicity is independent of which flavor quark pair is produced. In particular, we

expect a decrease of  $\langle n_{\text{had}} \rangle$  in  $e^+e^- \rightarrow \text{hadron}$  at the charm (or other heavy quark) threshold, but otherwise  $\langle n \rangle_{e^+e^- \rightarrow \text{had}} = n_{33}(s)$  will have a smooth monotonic increase with  $\log s$ .

This simple connection of color separation to hadron production implies that the same function  $n_{33}(s)$  controls the central region multiplicity in every process which begins with 3-3̄ separation, e.g., deep inelastic lepton scattering  $\ell p \rightarrow \ell' X$  ( $\ell q \rightarrow \ell q'$ ), and the Drell-Yan process  $A + B \rightarrow \ell \bar{\ell} X$  ( $q \bar{q} \rightarrow \ell \bar{\ell}$ ). See Fig. 15a,b,c. However, if a collision involves the separation of other color charges, e.g., color octet jets produced from initial gluon exchange or production of a gluon jet, then we predict a different, higher, rapidity height. There is also the intriguing possibility of color interference when several color systems are separated.

A crucial question in the above analysis is how to interpret the spectator system when a wee quark is removed from the hadron wavefunction. We shall assume that Fock space quarks tend to have similar velocities and rapidities in a bound state, and thus at the time of the interaction the spectator system can be regarded as a coherent 3̄ state with the rapidity of the initial hadron.<sup>12</sup> On the other hand, if one assumes that the wee quarks are the children of gluons in lowest order perturbation theory,<sup>9</sup> then the spectator system would consist of a color octet at the rapidity of the hadron, and a 3̄ at the rapidity of the struck quark. This argument seems tenuous, though, since the quark partons can exchange gluons over the indefinite time before the interaction. The role of gluon exchange in electroproduction is discussed further in the next section.

Given the simple 3̄ structure of the spectator wavefunction, we then are led to universal multiplicity plateaus in the current and hadron fragmentation regions of deep inelastic scattering, and the prediction that the multiplicity in  $\gamma^* p \rightarrow X$  is independent of  $q^2$  at fixed  $s = (q+p)^2$ —even for real photons. These results<sup>12</sup> are in apparent agreement with experiment.<sup>1</sup>

It is perhaps useful to briefly review the multiplicity calculations for QED.<sup>28</sup> The analogous problem to the color situation is the calculation to all orders in  $\alpha$  of the number of soft photons emitted by the outgoing muons in  $e^+e^- \rightarrow \mu^+\mu^-$ . The multiplicity is given by a Poisson distribution where  $\langle n_\gamma \rangle$  is determined simply by lowest order matrix

expression

$$\begin{aligned} \langle n_\gamma \rangle &= -\frac{e^2}{(2\pi)^3} \int_{k_{\min}}^{k_{\max}} \frac{d^3 k}{2k} \left( \frac{p_+^\nu}{p_+ \cdot k} - \frac{p_-^\nu}{p_- \cdot k} \right)^2 \\ &= \frac{\alpha}{2\pi} \left[ \frac{1}{\beta} \log \frac{1+\beta}{1-\beta} - 2 \right] \int_{k_{\min}}^{k_{\max}} \frac{dk}{k} \end{aligned} \quad (6.1)$$

Here  $\beta = [1-m^4/(p_+ \cdot p_-)^2]^{1/2}$  is the relative velocity of the pair and  $y = \frac{1}{2} \log \frac{1+\beta}{1-\beta}$  is the relative rapidity. A rapidity plateau arises naturally from the  $k \cdot p$  singularity of the angular integration near the light cone, and the  $dk/k$  integration serves to modify the height of the plateau. In QED,  $k_{\min} = 0$ , and  $\langle n_\gamma \rangle$  is logarithmically infinite. In QCD where there is eventual confinement, the gluons of very long wavelength ( $k_{\min}$  less than some hadronic size  $R^{-1}$ ) decouple since they only see an overall color singlet system and the multiplicity can be finite. Since  $k_{\max} \lesssim \sqrt{s}/\langle n_\gamma \rangle$ , we then have

$$\begin{aligned} \langle n_\gamma \rangle &= \frac{2\alpha}{\pi} \left( \log \frac{s}{m^2} - 1 \right) \log \frac{k_{\max}}{k_{\min}} \quad (s \gg m^2) \\ &\cong \frac{\alpha}{\pi} \log \frac{s}{m^2} \log \frac{s}{k_{\min}^2} \end{aligned} \quad (6.2)$$

where the hadronic  $k_{\min}^{-1}$  is the size of the color separation region. (In the model we discussed in Section III this region grows in proportion to  $\sqrt{s}$ .)

The result that the QED multiplicity (for  $k_{\min} \neq 0$ ) behaves as  $\log^2 s$  at high energies is somewhat surprising and perhaps deserves further comment. We first emphasize that this contribution is not dominated by the photons produced at large  $k_T$  relative to the charged lines.<sup>29</sup> Even if we were to impose a cutoff at  $k_T = k \sin \theta = k_{\max}$ , the angular integral still yields logarithmic form  $\int d\theta^2 / (\theta^2 + m^2/s) \sim \log s$ . The actual transverse momentum distribution of the photons is interesting: the infinite sum in  $\alpha$  falls off as a Gaussian<sup>30</sup> for moderate  $k_T^\gamma$  whereas at high  $k_T$ , the scale-invariant  $dk_T^2/k_T^2$  hard photon perturbation theory component takes over. Furthermore, the single photon distribution has a hint of the "seagull" effect. If we use light cone variables with  $x = (k_0 + k_3) / (p_0^+ + p_3^+)$ ,

$y = \log x + C$  then the leading  $p_+ \cdot p_-$  term in Eq. (6.1) gives

$$\frac{dN}{dk_T^2 dx} = \frac{\alpha/\pi}{k_T^2 + x^2 m^2} \frac{1}{\left[1 + \bar{k}_T^2 m^2 / (2xp_+ \cdot p_-)^2\right]} \quad (6.3)$$

Thus  $\langle \bar{k}_T^2 \rangle$  grows with  $x^2 m^2$  at small  $\bar{k}_T^2$ . Notice that in the central region (e.g.,  $x \sim 0 (m/\sqrt{s})$ ), the rapidity distribution is essentially flat, with  $dN/dy \sim \alpha/\pi \log s/k_T^2$  min.

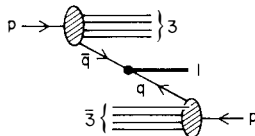
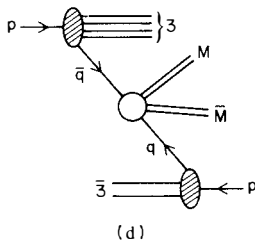
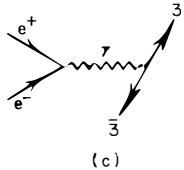
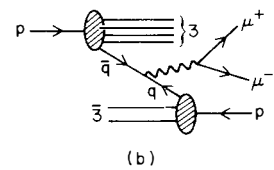
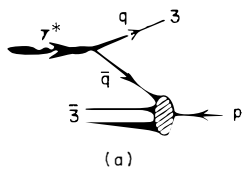
Chromodynamics is of course much more subtle and complicated than electrodynamics, and all we shall do here is argue that QED at least provides a covariant and consistent model for multiparticle production which may represent a pattern for gauge theories. We also note that the work of Ref. 31 suggests the possibility that the radiation of gluons in QCD may exponentiate into an effective Poisson form when gluons of the same order in the quark current are properly grouped together.

## VII. A Two Component Color Model

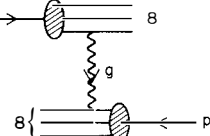
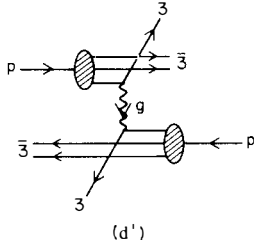
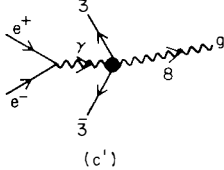
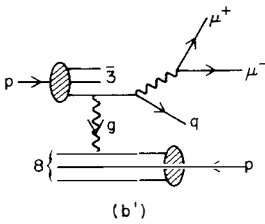
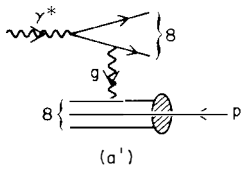
An intriguing feature, evident from the perturbation theory structure of QCD, is that all reactions can be classified according to whether the initial interaction separates a 3 and  $\bar{3}$  of color or separates octets of color. This is illustrated in Fig. 15 for (a) electro-production, (b) massive muon pair production, (c)  $e^+ e^-$  annihilation, (d) high  $p_T$  processes, and even (e) ordinary forward interactions. In each case only the initial interaction is shown; there is then subsequent gluon (and hadron) radiation which neutralizes the colored systems.

Using the color model<sup>12</sup> discussed in Section VI, we expect all of the reactions on the left side of Fig. 15 to have the identical plateau height  $dn/dy$  for rapidities in the central region between the separated 3 and  $\bar{3}$  systems. In fact all of the jet parameters  $\langle \bar{k}_T^2 \rangle$ , quantum number distributions, etc. should be indistinguishable in this region. In contrast to this we shall argue that whenever color octets are separated, the plateau height in the central region connecting their rapidities will be  $2\frac{1}{4}$  times as high:  $dn_{88}/dy = 9/4 dn_{3\bar{3}}/dy$ ; the number  $9/4 [=2/(1-n^{-2})$  in color  $SU(n)$ ] is derived from the lowest order perturbation graphs for gluon emission.<sup>12</sup> Roughly speaking, an octet has a color charge equal to  $3/2$  that of the triplet.

We can also give an intuitive argument which shows why octet separation leads to a rapidity height at least twice that of separating triplets.<sup>32</sup> Consider the gluon exchange

3- $\bar{3}$  SEPARATION

## OCTET SEPARATION



5-77

3191813

Fig. 15. Contributions to electroproduction, massive pair production,  $e^+e^-$  annihilation, large  $p_T$  hadron production, and forward hadronic collision, from both 3- $\bar{3}$  and octet-octet separation in color. In (e), the  $q\bar{q}$  can annihilate to a color singlet or a wee quark can be exchanged.

diagram in Fig. 15d' for a large  $p_T$  reaction. It is clear that there must be two neutralization chains connecting the top and bottom 3 and  $\bar{3}$ 's, and the multiplicity will be double that of electroproduction at the corresponding kinematics for  $3-\bar{3}$  separation, as in Fig. 15a. At low  $p_T$ , the same graph reduces to the Low<sup>20</sup>-Nussinov<sup>21</sup> model for the Pomeron, Fig. 15e', and the two neutralization loops will interfere. The interference is not destructive since that would correspond to color singlet exchange. Thus the resulting multiplicity plateau height must be at least double that of electroproduction or  $e^+e^- \rightarrow q\bar{q}$ . The QED analogue of this result would be positronium+positronium  $\rightarrow e^+e^-e^+e^-$  via photon exchange. For a high  $p_T$  collision the soft photon radiation has the usual plateau height along each outgoing lepton. At small  $p_T$  the interference of the radiation from different charged lines causes the plateau height to vanish in the case of photon exchange, but gives four times the height if the photon could transfer two units of charge. Notice that in the case of the color, the interference effect vanishes if  $n_{\text{color}} \rightarrow \infty$ .

It is possible that all hadron processes have both triplet- and octet-separation components, but that the latter is suppressed, at least at low energies, because of the extra associated multiplicity. Thus we speculate<sup>12</sup> that quark exchange and annihilation gives the dominant mechanism for massive pair production (Fig. 15b) (the Drell-Yan model) low multiplicity large  $p_T$  reactions (Fig. 15d) (the constituent interchange model), and by continuity to typical small  $p_T$  hadron reactions (wee quark exchange<sup>4,12</sup>). (See also the analysis of Section IV.) This ansatz, plus the color model, then can account for why the multiplicity plateau is observed to be essentially universal,<sup>2</sup> in all of these reactions.

On the other hand suppose we specifically consider events with high multiplicity, e.g., trigger only on events with at least double the usual hadron multiplicity. In this case the color octet diagrams on the right side of Fig. 15 will be favored, exposing the Berman, Bjorken, Kogut<sup>33</sup> gluon-exchange contribution for high  $p_T$  jets, and the Low-Nussinov gluon exchange mechanism for low  $p_T$  hadron reactions. Furthermore, a new essentially scale-invariant contribution from gluon exchange to  $pp \rightarrow \mu^+\mu^-X$  shown in Fig. 15b' will be dominant. (Notice that, unlike the Drell-Yan mechanism, this contribution gives the same production cross section for proton and antiproton beams.)

Similarly, the double multiplicity trigger in  $e^+e^- \rightarrow \text{hadrons}$  will enhance the  $e^+e^- \rightarrow q\bar{q}g$  contribution.

A two component color model for ordinary forward reactions automatically leads to a correlation between left and right hemisphere multiplicities of the type observed at the ISR<sup>34</sup>: the gluon exchange component will be dominant for events with a large rapidity plateau height  $dn/dy$  are considered, thus giving a large multiplicity throughout the central region.

Finally, we emphasize that by studying events with at least double the average multiplicity in  $pp$  collisions, one may be able to study  $qq \rightarrow qq$  scattering as it gradually evolves from the low  $p_T$  region (Fig. 15e') to high  $p_T$  scale-invariant jet production (Fig. 15d'). This can provide a nearly bias-free way of determining the jet-jet cross section.<sup>35</sup> Aside from its dependence on the effective coupling constant  $\alpha_s(p_T)$  we emphasize that the gluon exchange term is scale-invariant, and thus unlike quark exchange, does not contain a strong  $p_T$  cutoff of the forward jets.

### **VIII. Conclusions**

In this talk we have emphasized how the discrimination of various jet phenomena can determine the basic quark gluon mechanisms which control hadron dynamics. In particular, we have shown how quark, gluon, and multiquark jets can be distinguished by their retained quantum numbers, the leading-particle  $x$  dependence, and the multiplicity plateau height. A summary of representative jet parameters is given in Table I. Massive pair production reactions  $A + B \rightarrow \ell^+ \ell^- + X$  should be particularly interesting to study since the nature of the associated jets changes as one probes the wee and valence quark region. It is also interesting to study these quark and multiquark jet systems in a nuclear environment.

We have also emphasized the essential two-component nature of QCD and the relevant role of quark- and gluon-exchange mechanisms. In particular we have argued that wee quark exchange is the dominant hadron interaction at present energies. The ansatz that gluon exchange and production contributions can be made dominant by using a double multiplicity trigger could be an important phenomenological tool. Its confirmation would establish the dynamical role of color separation in multiparticle production.

Table I

Jet Type	Multiplicity	Example	Global Charge	Leading Particle	Typical Reactions
q	$n_{3\bar{3}}(s)$	u d	$\frac{2}{3} - \eta_Q$ $-\frac{1}{3} - \eta_Q$	$\pi^+, (1-x)$ $\pi^-, (1-x)$	current induced, large $p_T$ , Drell-Yan
qq	$n_{3\bar{3}}(s)$	$(uu)_3$	$\frac{4}{3} + \eta_Q$	$p, (1-x)$ $\pi^+, (1-x)^3$	quark exchange reactions, Drell-Yan, baryon spectators
gluon	$n_{88}(s)$	g	0	$M, (1-x)^2 \log s$ $B, (1-x)^4 \log s$	$e^+ e^- \rightarrow q\bar{q}g$ , $pp \rightarrow \gamma X$ , large $p_T$ , current induced
$B_8$	$n_{88}(s)$	$(uud)_8$	1	$p, (1-x)$ $\pi^+, (1-x)^5$	gluon exchange in hadronic reactions, $B + B \rightarrow X$
$M_8$	$n_{88}(s)$	$(u\bar{d})_8$	1	$\pi^+, (1-x)$ $p, (1-x)^5$	gluon exchange in hadronic reactions, $M + B \rightarrow X$
B	constant	p	1	$p, (1-x)^{-1}$ $\Lambda, (1-x)$ $\pi^+, (1-x)^5$	diffractive dissociation
M	constant	$\pi^+$	1	$\pi^+, (1-x)^{-1}$ $K^+, (1-x)$	diffractive dissociation

Acknowledgments

Most of this talk is based on work done in collaborations with R. Blankenbecler, W. Caswell, J. Gunion, R. Horgan, and N. Weiss. I am also grateful for discussions with M. Benecke, J. Bjorken, T. DeGrand, F. Low, and H. Miettinen.

## References

1. For a review and references, see S. J. Brodsky and J. F. Gunion, Proc. VII International Colloquium on Multiparticle Reactions, Tutzing (1976).
2. The multiplicity data are summarized in E. Albini *et al.*, Nuovo Cimento 32A, 101 (1976).
3. This section is based on work done in collaboration with N. Weiss. See S. J. Brodsky and N. Weiss, Stanford Linear Accelerator Center preprint SLAC-PUB-1926 (1977).
4. R. P. Feynman, Photon-Hadron Interactions (W. A. Benjamin, New York, 1972); Phys. Rev. Letters 23, 1415 (1969).
5. G. Farrar and J. Rosner, Phys. Rev. D 7, 2747 (1973). See also R. Cahn and E. Colglazier, Phys. Rev. D 9, 2658 (1974); J. L. Newmeyer and D. Sivers, Phys. Rev. D 9, 2592 (1974); D. Novseller, Phys. Rev. D 12, 2172 (1975).
6. R. D. Field and R. P. Feynman, Caltech preprint CALT-68-565 (1977).
7. J. Vander Velde, presented at the IV International Winter Meeting on Fundamental Physics, Salando, Spain (1976), University of Michigan preprint.
8. S. D. Drell and T.-M. Yan, Phys. Rev. Letters 25, 319 (1970).
9. V. A. Novikov, M. A. Shifman, A. I. Vainshtein, and V. I. Zakharov, preprint ITEP-112 (1976).
10. J. D. Bjorken, Proc. Summer Institute on Particle Physics, Stanford Linear Accelerator Center reports SLAC-167 and SLAC-PUB-1756 (1976). A. Casher, J. Kogut, and L. Susskind, Phys. Rev. Letters 31, 792 (1973).
11. R. Blankenbecler, S. J. Brodsky, and J. F. Gunion, Phys. Rev. D 12, 3469 (1975) and references therein.
12. S. J. Brodsky and J. F. Gunion, Phys. Rev. Letters 37, 402 (1976). I wish to thank T. DeGrand for discussions on color interference phenomena.
13. See also F. Low, XII Rencontre de Moriond (1977).
14. R. Blankenbecler and S. Brodsky, Phys. Rev. D 10, 2973 (1974). J. F. Gunion, Phys. Rev. D 10, 242 (1974). S. Brodsky and G. Farrar, Phys. Rev. Letters 31, 1153 (1973).

15. R. Blankenbecler and I. Schmidt, Stanford Linear Accelerator Center preprint SLAC-PUB-1881 (1977). See also S. Brodsky and B. Chertok, Phys. Rev. Letters 37, 269 (1976), and Phys. Rev. D 14, 3003 (1976).
16. R. Arnold et al., Phys. Rev. Letters 35, 776 (1975).
17. S. Brodsky and R. Blankenbecler, Ref. 14. See also H. Goldberg, Nucl. Phys. B44, 149 (1972).
18. J. C. Sens et al., quoted in W. Ochs, Nucl. Phys., to be published. F. E. Taylor et al., Phys. Rev. D 14, 1217 (1976). The  $p \rightarrow \bar{\Lambda}/p \rightarrow \Lambda$  ratio on nuclei is consistent with  $(1-x)^8$  or  $^9$ . O. Overseth, private communication and W. Ochs, XII Rencontre de Moriond (1977).
19. S. Brodsky and J. Gunion, Ref. 1 (and to be published). See also W. Ochs, XII Rencontre de Moriond (1977).
20. F. Low, Ref. 13, and Phys. Rev. D 12, 163 (1975).
21. S. Nussinov, Phys. Rev. Letters 34, 1286 (1973). See also J. F. Gunion and D. E. Soper, UC-Davis preprint (1976).
22. J. Ellis, M. K. Gaillard, and G. C. Ross, Nucl. Phys. B111, 253 (1976).
23. E. G. Floratos, CERN preprint TH-2261 (1976).
24. T. De Grand, Y. J. Ng, and S.-H. H. Tye, to be published.
25. D. Sivers and R. Cutler, to be published.
26. S. J. Brodsky, W. Caswell, and R. Horgan, in preparation.
27. S. Brodsky, C. Carlson, and R. Suaya, Phys. Rev. D 14, 2264 (1976).  
S. Brodsky, J. F. Gunion, and R. Jaffe, Phys. Rev. D 6, 2487 (1972).
28. D. R. Yennie, S. C. Frautschi, and H. Suura, Ann. Phys. 13, 379 (1961).
29. J. Dash, Marseille preprint (1977).
30. For a recent discussion, see G. Panchari-Srivastava and Y. Srivastava, North-eastern University preprint (1976).
31. J. M. Cornwall and G. Tiktopoulos, UCLA preprints TEP 2 (1976) and TEP 10 (1976). J. C. Taylor et al., XVIII International Conference on High Energy Physics, Tbilisi (1976) and J. Frenkel et al., Oxford preprint (1976).

32. Of course there is also the less interesting possibility that the result in QCD to all orders in perturbation theory (unlike QED) resembles thermodynamic models where the final state multiplicity has little to do with the initial process. I wish to thank J. Bjorken for conversations on this point.
33. S. Berman, J. Bjorken, and J. Kogut, Phys. Rev. D 4, 3788 (1971).  
J. Bjorken, Phys. Rev. D 8, 3098 (1973).
34. See M. Benecke, XII Rencontre de Moriond (1977); and M. Benecke, A. Bialas, and S. Pokorski, Nucl. Phys. B110, 488 (1976). I wish to thank M. Benecke for discussions on this point.
35. For an alternative method, see W. Ochs and L. Stodolsky, XII Rencontre de Moriond (1977).